

n-ZnO:Ga / p-Si heterojunction diodes grown by RF magnetron sputtering using powder target

B.Khalfallah, F.Chaabouni*, M.Abaab

Université Tunis El Manar - ENIT - Laboratoire de Photovoltaïque et Matériaux Semiconducteurs, BP 37, Le belvédère
1002 (TUNIS)

E-mail: fchaabouni@yahoo.fr

ABSTRACT

Thin films of undoped and Ga-doped ZnO with different doping concentrations (0, 3, 5, 7 wt.%) were deposited on (100) silicon substrates by RF magnetron sputtering using a powder target. The results show that the devices have good rectifying behaviors with an ideality factor values in the range of 1.16-1.81 and a barrier height values in the range of 0.60-0.64 eV based on the $I-V$ characteristics. Also, Cheung's functions were used to estimate the series resistance of the diode. From the $C-V$ characteristics, it is shown that the capacitance increases with decreasing frequencies. $C-V$ measurements give higher barrier than those obtained from $I-V$ measurements. The results demonstrate that the structural and electrical properties of ZnO/p-Si heterojunction diodes are controlled by the Ga dopant content. © 2014 Trade Science Inc. - INDIA

KEYWORDS

GZO thin films;
RF sputtering;
I-V measurements;
C-V measurements;
Barrier height.

INTRODUCTION

As a potential transparent conductive oxide (TCO) substituting the most commonly used but expensive materials such as ITO and SnO_2 , ZnO has attracted great attention in the last decades. Indeed, ZnO offers interesting properties such as stability in hydrogen plasma commonly used in the fabrication of amorphous silicon solar cells, non-toxicity and good adherence to many substrates^[1]. Group III elements such B, In, Al and Ga are usually used to improve the conductivity of ZnO. Due to its similar ionic radius and the covalent bond length, Ga doping brings about only a small lattice deformation even for a high Ga concentration^[2]. Furthermore, Ga is less reactive and more resistive to oxidation than Al during the deposition^[3], so Ga doped

ZnO is getting more and more attention recently. Various ZnO-based heterojunction devices have been fabricated using different p-type substrate materials such as GaN^[4], PFO polymer^[5] and 4H-SiC^[6]. Silicon already has a central position in the microelectronics industry, with several advantages such as high quality, large area p-type substrates available at low cost.

In this paper, Ga-doped ZnO thin films were prepared on Si substrate by radio-frequency magnetron sputtering technique with different Ga contents and the n-p heterojunction properties by means of the current-voltage ($I-V$) and capacitance-voltage ($C-V$) measurements were studied.

EXPERIMENTAL

ZnO and ZnO: Ga films were deposited on silicon

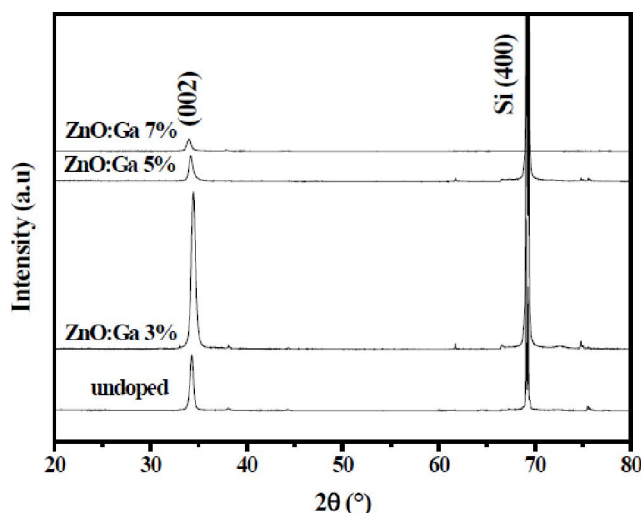


Figure 1: XRD diagram of pure and Ga doped ZnO thin films

substrate at room temperature using RF magnetron sputtering. The Si substrates used in this study were p-type single crystal (100) with a thickness of 500 μm and a resistivity of 50 Ωcm . Si substrates were cleaned ultrasonically in acetone for 15 min, rinsed with deionized water and then were dried. Ga_2O_3 (99.99%) powder was added to a ZnO (99.99%) powder target as dopant. The powder was lightly tamped down on a 4 in. diameter copper backing plate to produce a uniform thickness (4 in.) and surface to target distance. No further processes such as sintering were involved in target production. The Ga doping ratio was adjusted at 3, 5 and 7 wt. %. The substrates were rotated (15 rd/mn) and placed parallel to the target surface at a distance of 65 mm. RF magnetron sputtering power density was adjusted to 2.5 W/cm^2 . In order to avoid film's contamination, the chamber was evacuated to a base pressure of about 10^{-4} Pa. Argon (Ar) gas was introduced into the chamber through a mass flow controller. The mass flow of argon gas was fixed at 3 sccm, corresponding to a final pressure of 0.6 Pa.

The structure properties of the films were analyzed by X-ray diffraction (PANalytical X'Pert Pro, Philips Co, Ltd) with $\text{Cu K}\alpha$ radiation ($\lambda = 0.15406$ nm), to identify the crystal structure and orientation of each phase. ASTM table were used for indexing the lines. Surface morphology was observed using an atomic force microscope (Nanoscope IIIa Veeco type dimension 3100). Capacitance-Voltage ($C-V$) measurements were performed with the impedance analyzer HP 4192A, to determine the built-in potential of ZnO/p-Si

and ZnO:Ga/p-Si heterojunctions and current voltage characteristics ($I-V$) of the heterojunctions were measured at room temperature by using the DC voltage-current source unit (Agilent N6762A). Ohmic contacts of silver paste were applied onto the ZnO:Ga films as the top electrode and to the p-silicon substrate as the bottom electrode. Film thickness was estimated with Swanpoel method^[7], based on the use of the interference fringes extremes of the transmittance and reflectance spectra, applied on ZnO:Ga films deposited on glass samples grown simultaneously with the ZnO:Ga/Si films.

RESULTS AND DISCUSSION

Structural properties

XRD pattern of ZnO:Ga films deposited on silicon substrate with different Ga doping contents is shown in Figure 1 (the film thickness is 580 nm in average).

A weak ZnO (002) and very strong Si(400) substrate diffraction peaks were observed for the deposited ZnO film. All films were polycrystalline with a hexagonal wurtzite structure and a preferred orientation with the c-axis perpendicular to the substrate; no phases corresponding to Ga_2O_3 were detected. With a Ga-doping content of 3 wt. %, the intensity of the (002) peak and Si(400) substrate diffraction peaks increased, indicating an improvement in the crystallinity. With further Ga-doping content up to 7 wt. %, the intensity of (002) peak decreased. This behavior is congruent to the classical Al and In doping effect on the ZnO structure^[8-10]. In these cases, the doping atoms destroy the initial preferential orientation of the undoped film, with increasing the doping concentration the film becomes polycrystalline and the textured structure disappears^[11]. The (002) peak position was linearly shifted to the lower 2θ value with the increase of Ga content. This shift indicates that the films are in a uniform state of stress with tensile components parallel to c-axis. Similar shifts were also observed in ZnO:Al films in previous studies^[12,13]. This result could be attributed to an enhancement of the crystallinity and the possibility of replacing zinc ions (Zn^{2+} : 0.74 Å) by the gallium ions (Ga^{3+} : 0.62 Å) of the host matrix, which create the lattice strain and consequently modified the lattice parameters.

The microstrain ε in ZnO thin films along c-axis

TABLE 1: Structural parameters obtained from XRD pattern

Samples	ZnO	ZnO:Ga 3 %	ZnO:Ga 5 %	ZnO:Ga 7 %
(002) peak position in 2θ terms ($^\circ$)	34.31	34.23	34.12	34.00
FWHM ($\beta_{(002)}$ ($^\circ$))	0.317	0.250	0.329	0.338
Grain size D (nm)	26.20	33.15	26.00	24.60
Lattice parameter (\AA)	5.225	5.230	5.253	5.271
Stress (GPa)	-0.881	-0.411	-2.144	-2.950

perpendicular to the substrate was calculated using the equation:

$$\varepsilon = \frac{\Delta c}{c_0} \quad (1)$$

where Δc is the difference between the lattice parameter ' c ' of the films (calculated from XRD data) and the lattice parameter ' c_0 ' of unstrained ZnO (0.5206 nm)^[14]. The estimated values of this stain is about 10^{-3} , this result may be caused by a tensile stress due to Zn^{2+} ions substitution by Ga^{3+} ions in the lattice. The residual stress σ in the plane of the film can be calculated from the strain with the biaxial strain model^[14]:

$$\sigma = \frac{2C_{13}^2 - C_{33}(C_{11} + C_{12})}{C_{13}} \times \varepsilon \quad (2)$$

where C_{ij} are the elastic stiffness constants for single ZnO crystal ($C_{11} = 208.8$ GPa, $C_{33} = 213.8$ GPa, $C_{12} = 119.7$ GPa, $C_{13} = 104.2$ GPa)^[15,16]. Equation 3 can be simplified to $\sigma_{\text{film}} = -233 \times \varepsilon$ (GPa). Stress values for ZnO:Ga films at different doping concentration were listed in TABLE 1. The negative stress values indicated that the films were in a state of compressive stress.

The grain size can be accessed by the XRD data using the Debye–Scherrer formula^[15]:

$$D = \frac{0.9\lambda}{\beta \cos \theta} \quad (3)$$

where D is the average grain size, λ is the X-ray wavelength, θ is the diffraction angle of the peak and β is the FWHM. The calculated grain size with different doping concentrations is shown in TABLE 1. It was found that the 3 wt. % Ga-doped films have the largest value of grain sizes. Therefore, the film deposited under the Ga content of 3 wt. % has the best structural properties. However, as the Ga content increases from 3 to 7 wt.%, the grain sizes decreases, which indicate, that higher content of Ga leads to a deterioration of the crystal

structure by distorting the ZnO lattice. Compressive stress values increased as the Ga content increases. This result could be related the occupancy of Ga ions in the interstitial sites of ZnO for higher Ga doping concentrations^[17,18]. The length of c-axis in the films was calculated from the equation of hexagonal structure interplanar spacing. The results are shown in TABLE 1. It is found that the length of c-axis increases with increasing Ga content, which indicated that the residual stress and lattice constant in ZnO films changed^[19]. It can be concluded from the results that an appropriate Ga doping in the ZnO films can improve the structural properties of the ZnO films.

Surface morphology

Figure 2 displays the AFM micrographs ($2 \mu\text{m} \times 2 \mu\text{m}$) of the ZnO films for various Ga concentrations.

It can be seen that all samples demonstrates a uniform and densely packed granular arrangement. Indeed, the images indicate a correlation between Ga concentration and surface morphology by means of different crystallite sizes. The increase in the doping concentration tends to produce changes in the crystallite size and the surface roughness. The roughness decreases as a result of crystallites size decrease^[20]. For the scanning area ($2 \mu\text{m} \times 2 \mu\text{m}$), the root-mean squares (RMS) of average surface roughness are determined as 12.25, 16.55, 15.75 and 8.50 nm for undoped and Ga-doped ZnO thin films of 3 wt.%, 5 wt.% and 7 wt.%, respectively. It was found that the 3 wt. % Ga-doped films have the highest value of surface roughness which is consistent with the XRD results shown above.

Electrical properties

(a) I – V characteristics of undoped and Ga-doped ZnO/p-Si heterojunction

The current–voltage (I – V) characteristics of undoped and Ga-doped ZnO/p-Si heterojunction di-

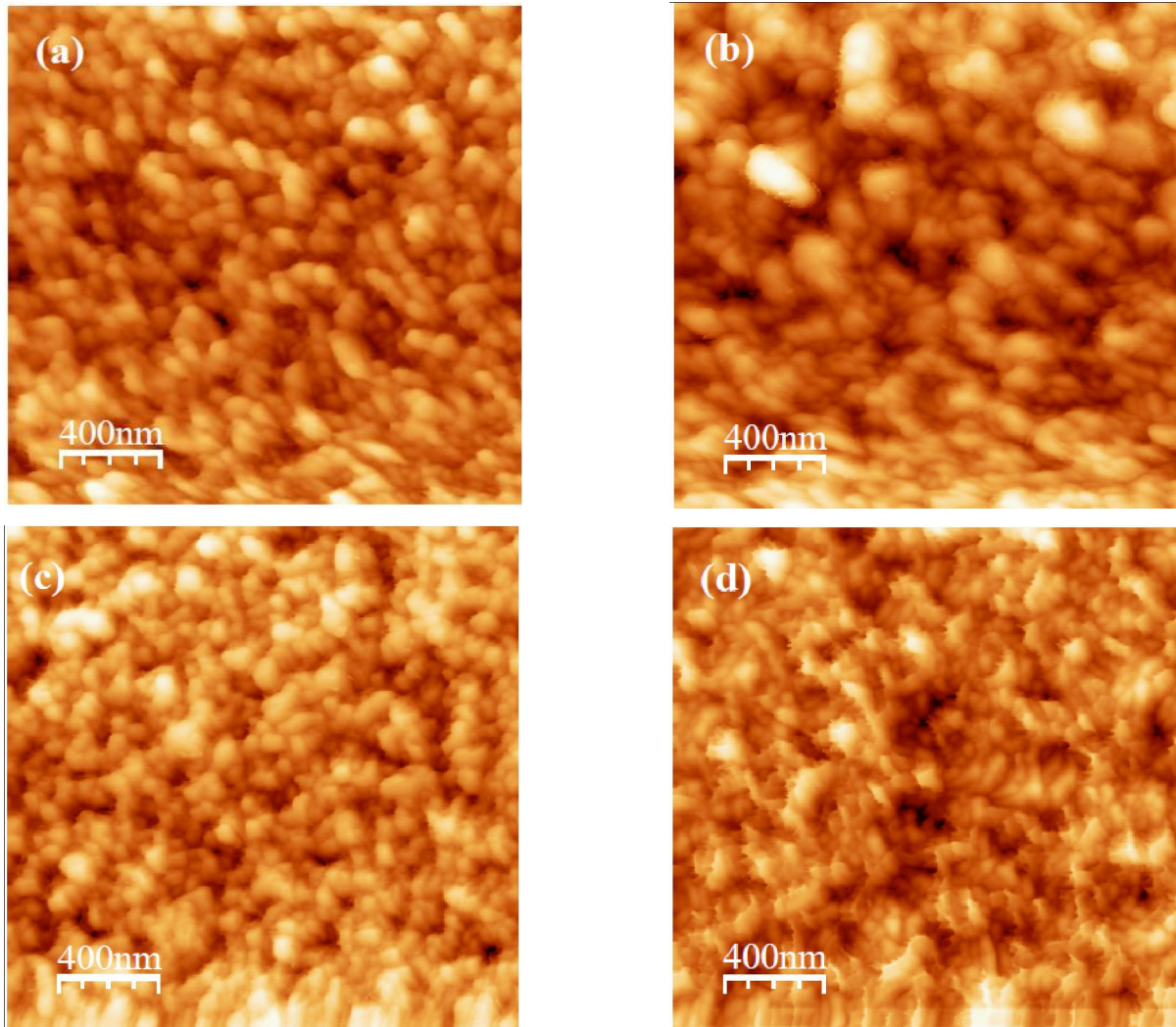


Figure 2: AFM images of ZnO:Ga films with Ga contents of (a) 0 wt.%, (b) 3 wt.%, (c) 5 wt.% and (d) 7 wt.%

TABLE 2 : Electrical parameters obtained from I-V and C-V measurements

	I-V measurements				C-V measurements		
	n	I_s (A)	θ (eV)	R_s (Ω)	V_{bi} (V)	N_D (cm^{-3})	θ (eV)
Undoped	1.16	$4.11 \cdot 10^{-5}$	0.63	49.03	0.70	$9.54 \cdot 10^{15}$	0.85
ZnO:Ga 3 wt.%	1.81	$7.17 \cdot 10^{-6}$	0.64	57.01	0.67	$5.22 \cdot 10^{16}$	0.77
ZnO:Ga 5 wt.%	1.79	$1.57 \cdot 10^{-5}$	0.61	10.06	0.71	$1.39 \cdot 10^{18}$	0.73
ZnO:Ga 7 wt.%	1.74	$2.4 \cdot 10^{-5}$	0.60	27.13	0.72	$7.04 \cdot 10^{17}$	0.76

ode measured at room temperature are shown in Figure 3.

The I - V characteristics of the structures shows good rectification and were plotted to determine the barrier height and the ideality factor of the diodes. For voltages higher than $3kT/q$, the $\ln(I)$ - V plot show a linear region which can be used to determine the values of the ideality factor and barrier height. The standard diode equation is given by^[21]:

$$I = I_s \left[\exp\left(\frac{q(V - IR_s)}{nkT}\right) - 1 \right] \quad (4)$$

where R_s is the series resistance, n is the ideality factor and I_s is the saturation current derived from the straight line intercept of $\ln(I)$ at $V = 0$ and is given by:

$$I_s = A^* AT^2 \exp\left(-\frac{q\phi_B}{kT}\right) \quad (5)$$

Full Paper

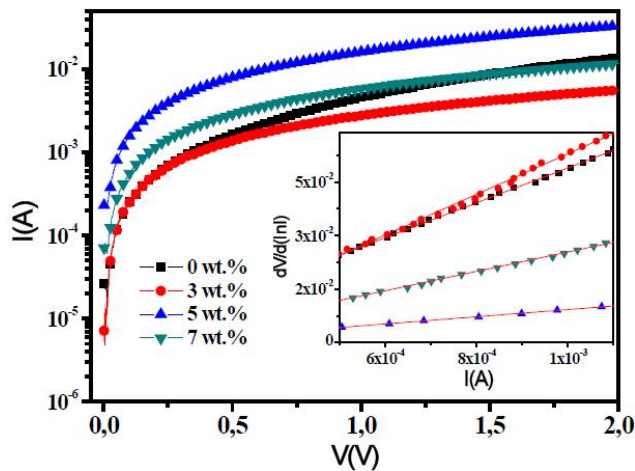


Figure 3: Current–voltage characteristics at room temperature of undoped and Ga-doped ZnO on p-Si substrates. The inset is $dV/d(\ln I)$ vs. I plot of the deposited films

where q is the electron charge, V is the definite forward bias voltage, A is the contact area, A^* is the effective Richardson constant (for n-ZnO, $A^* = 32 \text{ K}^2 \text{ cm}^{-2}$ [22]), k is the Boltzmann constant, T is absolute temperature and Φ_B is the barrier height. Thus, the barrier height can be obtained from the equation:

$$\Phi_B = kT \ln \left(\frac{A A^* T^2}{I_s} \right) \quad (6)$$

The barrier height of undoped and Ga-doped ZnO/p-Si heterojunction is around 0.60 eV. This value is in good agreement with that obtained for ZnO/p-Si prepared by DC sputtering (0.69 eV)[23] and lower than that obtained in our previous study for a ZnO/p-Si diode fabricated by RF sputtering technique[24].

The ideality factor was determined from the slope of the linear region of the forward bias $\ln(I)$ – V characteristic through the relation:

$$n = \frac{q}{kT} \frac{dV}{d(\ln I)} \quad (7)$$

The values of the ideality factor are greater than unity, as show in TABLE 2, which implies derivation from ideal behavior.

Thus, this result can be attributed to the interfacial thin native oxide layer at the Ag and ZnO interface and the series resistance effect. The ideality factor increases with the Ga content up to 3 wt. % then decreases, indicating a variation in recombination component due to the additional defects introduced by Ga incorporation, and/or the series resistance effects.

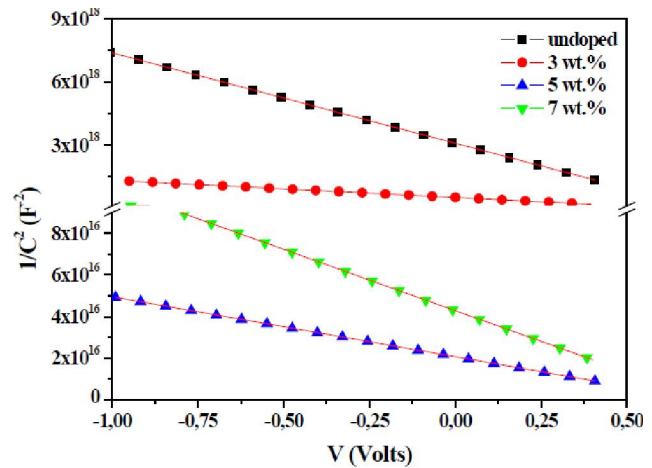


Figure 4: The reverse-bias C^{-2} – V characteristics of undoped and Ga-doped ZnO on p-Si substrates

The series resistance R_s can also be obtained using a method developed by Cheung and Cheung[25], using the following function:

$$\frac{dV}{d(\ln I)} = IR_s + \frac{nkT}{q} \quad (8)$$

The inset in Figure 3 shows a linear plot of $dV/d(\ln I)$ vs. I of un-doped and Ga-doped ZnO/p-Si heterojunction. R_s is determined as the slope of the $dV/d(\ln I)$ vs. I plot. The values of R_s have been calculated and summarized in TABLE 2. These values may be affected by the inhomogeneity of the contacts during the elaboration.

(b) C – V characteristics of undoped and Ga-doped ZnO/p-Si heterojunction

The potential barrier at the junction can be measured by small-signal capacitance–voltage (C – V) characteristics. The capacitance measurements were performed at room temperature at a frequency of 100 kHz under applied forward and reverse DC bias sweeps (~ 10 to 10 V) with an AC oscillation level of 0.5 mV. The depletion region capacitance can be written as[26]:

$$C^2 = \frac{qN_D N_A \epsilon_1 \epsilon_2}{2(\epsilon_1 N_D + \epsilon_2 N_A)} \frac{1}{(V_{bi} - V)} \quad (9)$$

where N_D and N_A are donor density in n-ZnO and acceptor density in p-Si, and ϵ_1 and ϵ_2 are dielectric constants of n-ZnO and p-Si, respectively and V is the applied voltage.

For an applied reverse voltage $V \gg kT/q$, and knowing that $N_A \gg N_D$, the relationship between the depletion layer capacitance per unit area and the ap-

plied voltage is given by:

$$\frac{1}{C^2} = \frac{2(V_{bi} - V)}{q\epsilon_s\epsilon_0 S^2 N_D} \quad (10)$$

with ϵ_s is the dielectric constant of the semiconductor ($\epsilon_s\epsilon_0 = 7.965 \times 10^{-11}$ F/m^[27], $\epsilon_0 = 8.85 \times 10^{-12}$ F/m is the dielectric constant of vacuum, V_{bi} is the diffusion potential at zero bias determined from the extrapolation of the linear reverse bias C^{-2} - V plot. The barrier height is given by the following equation:

$$\Phi = qV_{d0} + kT \ln \left(\frac{N_c}{N_D} \right) \quad (11)$$

The diffusion voltage at zero bias, V_{d0} , is equal to $V_{bi} + kT/q$ where $kT/q \ln(N_c/N_D)$ represents the depth of the Fermi level below the conduction band in the neutral region of the semiconductor. N_c is the density of states in the conduction band, which is $N_c = 3.5 \times 10^{18}$ cm⁻³ for ZnO at room temperature^[26].

Figure 4 depicts the C - V measurements of undoped and Ga-doped ZnO/p-Si heterojunction. The C^{-2} vs. V relationship was linear, which confirmed the formation of a heterojunction at the n-ZnO/p-Si interface.

Under reverse bias conditions, the capacitance decreased as the reverse bias increased. The donor concentration of undoped and Ga-doped ZnO/p-Si heterojunction was calculated from the slope and the barrier height estimated from the extrapolated intercept of $1/C^2$ with the voltage axis. The calculated values of carrier concentration and barrier height of undoped and Ga-doped ZnO/p-Si heterojunction are summarized in TABLE 2. It was found that the values of the barrier height extracted from the C - V curves are higher than those derived from the I - V measurements. This difference can be due to an interface layer and the barrier inhomogeneities^[28]. The potential height decreases with the Ga-doping content, and is around 0.70 eV. This value is consistent with the energy difference of the work functions between Si and ZnO; the Fermi level below the vacuum level is 4.97 eV for p-Si and 4.25 eV for ZnO, and the difference between them is 0.72 eV. The donor concentration increases with the Ga-doping content level as preview but decreases for the Ga content of 7 wt.%. This decrease effect can be interpreted as a structural reorganization of the sample (7 wt.%), which was confirmed by the structural analysis.

CONCLUSION

High quality ZnO and ZnO:Ga thin films on a Si substrate have been grown by RF magnetron sputtering using a powder target. X-ray diffraction study showed that the structure of the film is hexagonal with a strong (002) preferred orientation. The film deposited under the Ga content of 3 wt. % revealed the best structural properties. The device current-voltage curve showed excellent rectification behaviors. The ideality factor of the heterojunction was obtained from curve fitting and found to be in the range of 1.16 and 1.81 and the barrier height values were around 0.60 eV. It was found that the barrier height values obtained from the C - V measurements are higher than those obtained from I - V measurements. The electrical performance of ZnO/p-Si heterojunction diodes can be controlled by the Ga dopant content. The results indicate that ZnO:Ga/p-Si heterojunctions are good candidates for electronic device applications.

REFERENCES

- [1] O.Kluth, B.Rech, L.Houben, S.Wieder, G.Schope, C.Beneking, H.Wagner, A.Loffl, H.W.Schock; *Thin Solid Films*, **351**, 247 (1999).
- [2] V.Assuncao, E.Fortunato, A.Marques, H.Aguas, I.Ferreira, M.E.V.Costa, R.Martins; *Thin Solid Films*, **427**, 401 (2003).
- [3] L.Fang, K.Zhou, F.Wu, Q.L.Huang, X.F.Yang, C.Y.Kong; *J Supercond Nov Magn.*, **23**, 885 (2010).
- [4] S.P.Chang, R.W.Chuang, S.J.Chang, Y.Z.Chiou, C.Y.Lua; *Thin Solid Films*, **517**, 5054 (2009).
- [5] A.Zainelabdin, S.Zaman, G.Amin, O.Nur, M.Willander; *Nanoscale Res. Lett.*, **5**, 1442 (2010).
- [6] N.Bano, I.Hussain, O.Nur, M.Willander, P.Klason, A.Henry; *Semicond. Sci. Technol.*, **24**, 125015 (2009).
- [7] R.Swanpoel; Determination of the thickness and optical constants of amorphous silicon, *J. Phys. E*, **16**, 1214 (1983).
- [8] Mujdat Caglar, Saliha Ilican, Yasemin Caglar; *Thin Solid Films*, **517**, 5023 (2009).
- [9] G.Kenanakis, N.Katsarakis, E.Koudoumas; *Thin Solid Films*, **555**, 62 (2014).
- [10] Y.S.Zou, H.Yang, H.P.Wang, D.Lou, C.J.Tu, Y.C.Zhang; *Physica B*, **414**, 7 (2013).

Full Paper

- [11] A.Mhamdi, B.Ouni, A.Amlouk, K.Boubaker, M.Amlouk; *Journal of Alloys and Compounds*, **582**, 810 (2014).
- [12] O.Baka, A.Azizi, S.Velumani, G.Schmerber, A.Dinia; *J Mater Sci: Mater Electron*, **25**, 1761 (2014).
- [13] H.Gomez, M.de la L.Olvera; *Materials Science and Engineering B*, **134**, 20 (2006).
- [14] H.C.Ong, A.X.E.Zhu, G.T.Du; *Appl. Phys. Lett.*, **80**, 941 (2002).
- [15] D.Cullity; "Elements of X-Ray Diffraction", 2nd Edition, Addison-Wesley; Reading, USA (1978).
- [16] F.Conchon, P.O.Renaul, E.Le Bourhis, C.Krauss, P.Goudeau, E.Barthel, S.Yu.Grachev, E.Sondergard, V.Rondeau, R.Gy, R.Lazzari, J.Jupille, N.Brun; *Thin Solid Films*, **519**, 1563 (2010).
- [17] Quan-Bao Ma, Zhi-Zhen Ye, Hai-Ping He, Shao-Hua Hu, Jing-Rui Wang, Li-Ping Zhu, Yin-Zhu Zhang, Bing-Hui Zhao; *Journal of Crystal Growth*, **304**, 64 (2007).
- [18] Hyunsik Yoon, Soaram Kim, Hyunggil Park, Giwoong Nam, Yangsoo Kim and Jae-Young Leem; *Journal of the Korean Physical Society*, **64**, 109 (2014).
- [19] J.J.Ding, H.X.Chen, S.Y.Ma; *Physica E*, **42**, 1861 (2010).
- [20] V.Khranovskyy, U.Grossner, O.Nilsen, V.Lazorenko, G.V.Lashkarev, B.G.Svensson, R.Yakimova; *Thin Solid Films*, **515**, 472 (2006).
- [21] E.H.Rhoderick, R.H.Williams; "Metal-semiconductor Contacts", 2nd ed., Clarendon Press; Oxford (1988).
- [22] H.von Wenckstern, E.M.Kaidashev, M.Lorenz, H.Hochmuth, G.Biehne, J.Lenzner, V.Gottschalch, R.Pickenhain, M.Grundmann; *Appl. Phys. Lett.*, **84**, 79 (2004).
- [23] L.Shen, H.W.Du, H.Ding, J.Tang, Z.Q.Ma; *Materials Science in Semiconductor Processing*, **13**, 339 (2010).
- [24] F.Chaabouni, M.Abaab, B.Rezig; *Superlattices and Microstructures*, **39**, 171 (2006).
- [25] S.K.Cheung, N.W.Cheung; *Appl. Phys. Lett.*, **49**, 85 (1986).
- [26] S.M.Sze; "Physics of Semiconductor Devices", 2nd Edition., Wiley; New York (1981).
- [27] H.Sheng, S.Muthukumar, N.W.Emanetoglu, Y Lu; *Appl. Phys. Lett.*, **80**, 2132 (2002).
- [28] S.Aydogan, K.Cýnar, H.Asýl, C.Coskun, A.Turut; *Journal of Alloys and Compounds*, **476**, 913 (2009).